Proceedings of the IEEE-EMBS International Conference on Biomedical and Health Informatics (BHI 2012)
Hong Kong and Shenzhen, China, 2-7 Jan 2012

Arterial Pressure Pulse Palpation with the Haptic Lens

Mahsan Rofouei, Pooya Monajemi, Mike Sinclair and Majid Sarrafzadeh

Abstract—**Palpation is a traditional method for diagnosis that uses the sense of touch. Due to its subjective nature, results from palpation are not always accurate and/or consistent. Therefore in order to enable a consistent and quantitative analysis by palpation, we propose this diagnostic by a novel device called the Haptic Lens. Considering the richness of parameters in the cardiac pressure pulse, we focus on developing a quantitative method for measuring arterial pressure pulse parameters using the Haptic Lens. We develop algorithms that enable accurate measurements of arterial pulse parameters. To demonstrate the efficacy of our approach and the ease of learning this method we used this device to measure arterial pulse parameters on 10 individuals.**

I. Introduction

PALPATION is a traditional diagnostic procedure in which physicians use their fingers to externally touch and feel body tissues. It is used as part of a physical examination to determine the spatial coordinates of an anatomical landmark, assess tenderness through tissue deformation and determine size, shape, firmness or location of an abnormality in the body through the tactile sensing of elasticity modulus differences. It can be used in finding tumors, arteries, moles, etc. It can also be used to diagnose edema and to measure the pulse.

An arterial pulse pressure waveform is considered to be a fundamental indicator for diagnosis of several cardiovascular diseases. An arterial pulse waveform can be acquired by palpation on different areas on the body such as finger, wrist, foot and neck.

The waveform acquired by palpation is considered to offer more information than the single pulse waveform from an electrocardiogram (ECG). The ECG signal only reflects bio-electrical information of the body while a pulse palpation signal, especially at different locations along the artery, reveals diagnostic information not visible in ECG signals [2].

In addition, pulse palpation has been used as a fundamental diagnostic method in Traditional Chinese Medicine (TCM) [2]. Diagnostic features such as width, strength (amplitude), pulse rate, pulse length and shape (amplitude vs. time) variations can be extracted through pulse palpation on a location situated next to the prominent bone on the wrist.

Manuscript received October 14, 2011. Mahsan Rofouei is with University of California, Los Angeles (phone: 310-267-5243; e-mail: mahsan@cs.ucla.edu). Pooya. Monajemi, is with University of California, Los Angeles, (e-mail: pmonajemi@ucla.edu). Mike. Sinclair is with Microsoft Research, Redmond (e-mail: sinclair@microsoft.com). Majid sarrafzadeh is with University of California, Los Angeles. (email: majid@cs.ucla.edu).

Palpation is subjective where the results may vary among physicians. It can be extremely dependent on the physician's ability and experience which makes the results prone to error.

Our solution to this problem is the Haptic Lens [1]. The Haptic Lens is a low-cost device that enables the real-time visualization of the haptic sense of elastic modulus boundaries which is essentially the tissue deformation caused by a specific force. Within the Haptic Lens, images are captured that describe the 3D position and movement of underlying tissue during the application of a known force – essentially what a physician feels through manual palpation. The device and supporting software enable the visualization and documentation of the equivalent of 3D tactile input from a known applied force. The Haptic Lens can eliminate the subjective analysis of physical palpation examinations and give more accurate and repeatable results, yet is less expensive to implement than MRI, ultrasound or similar techniques.

Data processed from captured images is also a good means for documentation for patient records. This way, physicians may also be able to objectively measure change over time by comparing past data. By incorporating image registration techniques, accurate assessment of change over time is possible. Physicians can also share extracted features of abnormalities, etc. together with captured images and data among other physicians for further research.

Another application of the Haptic Lens is in teaching medical palpatory diagnosis. Recently, new haptic technology is becoming promising in medical training. As an example the Virtual Haptic Back (VHB) is a virtual reality tool of the human back for teaching clinical palpatory diagnosis [8]. Less experienced physicians or medical students can enhance their palpation perception by comparing their assessments with accurate quantitative assessments from the Haptic Lens.

The Haptic Lens can also help move towards virtual palpation. It can be used to develop applications such as remote diagnosis of medical conditions for use in rural locations. Based on the advantages of such a device, it is important to design a device which captures accurate information that the haptic sense of human administered palpation would. The goal in this work is to develop a quantitative approach for capturing and analyzing arterial pulse pressure waveform in a non-invasive, low cost and easy to learn approach. The rest of the paper is organized as follows: In section II we provide a brief overview of related work in this area. Section III describes different components

978-1-4577-2177-9/12/$25 (C) 2012 IEEE

of the Haptic Lens device used for data acquisition. Following it in Section IV we describe preliminaries on arterial pulse parameters. The detail of data processing is described in Section V and experimental results are show in Section VI. Finally conclusions and future work are described in section VII.

II. Related Work

Different acquisition systems and devices have been developed for measuring human cardiac signals. The Doppler ultrasound sensor uses reflected sound waves to monitor blood flow through blood vessels [4]. Wu, et al [3] uses a laser triangulation method to detect skin vibrations. Other methods such as thermal imaging [7], pressure [5] and acoustic-based [6] sensors have also been explored.

The main disadvantage of most of the aforementioned methods is that they involve relatively large devices for capturing pulse waveforms and require a person with knowledge about the system to work with them. Our approach is very similar to the natural palpation procedure where fingers are pressed into the palpatory area. The device is pressed against the palpatory area and the pulse signal is immediately visualized so that the individual can reposition the device until a clear pulse is captured. In addition, when comparing with pressure sensor based methods which use either a single sensor or sensor arrays (9 sensors in [5]) our approach increases the accuracy to the pixel level. Our proposed method is also portable, non-invasive and low cost.

III. Device

Figure 1 shows the structure and different parts that compose the Haptic Lens: a white deformable membrane, isotropically died elastomer or liquid; a clear rigid face plate; an illumination source; and a camera.

Fig. 1. Haptic Lens Components.

The Haptic Lens functions in the following way: The object of interest (in this case an individual's wrist) is pressed externally against the white membrane of the Haptic Lens. This results in the 3D deformation of the membrane and the contained dyed elastomer and finally in the grayscale image representing the 3D depth map of the applied object captured by the camera. Different parts of the object are deformed at different depths from the faceplate, proportional to the local applied force and inversely by the object's modulus. This 3D deformation of the optically attenuating elastomter causes the illumination to pass through varying thicknesses and hence varying attenuations as seen by the camera. The less the distance of elastomer the light has to travel through, the lighter it appears. Therefore positions on the reflecting white membrane which are deformed to be nearer to the face plate appear lighter than positions further away. This results in a function that maps membrane deformation "heights" at each pixel location to the camera's grayscale intensity value at that location. This is a sensor that acts like a real-time 3D surface digitizer. It should be noted that a dyed liquid can be used in place of the elastomer.

IV. Arterial Pulse Characteristics

There are different kinds of pulse patterns defined based on different criteria such as position, rhythm, shape, etc. From shape perspective all these pulses can be defined according to presence or absence of three types of waves. These three waves are: (1) P (percussion or primary) wave, (2) T (Tidal or secondary) wave and (3) D (Dicrotic or triplex) wave [9, 10]. Examples of one segment pulses with the presence or absence of these waves are shown in Fig 2.

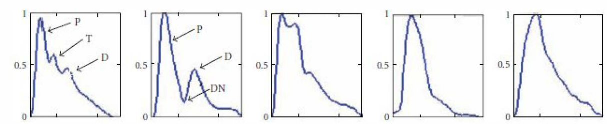

Fig. 2. Different pulse shapes from [9]: Amplitude vs Time.

The percussion, tidal and dicrotic waves can be indicators of specific conditions. For example they can indicate the decrease in the compliance of small arteries and the elasticity of blood vessel wall [11]. In addition to the shape of the pressure pulse features such as width and rate, the position of the pulse is also important. Measuring pulse propagation time along the artery is also important in measuring blood velocity. With the current sampling rate of 60Hz this feature is not available but we believe the Haptic Lens has the ability to demonstrate this at higher sampling rates.

V. Signal Processing and Feature Extraction

Data is collected from the image sensor at a rate of 60 fps, with a frame resolution of 640 by 480 pixels. In the interest of lowering the computational complexity of the algorithm, the frame size is down-sampled to 128 by 96 pixels. Furthermore, an initial "empty" frame is used to subtract unwanted artifacts from the images.

In the next step a 3D baseline removal procedure is performed. Baseline drift is visible in raw data. This is due to applied pressure variation from human movement. Multiple schemes are available for advanced baseline removal procedures, however it was experimentally determined that a simple time domain high pass filtering with a cut off frequency of 0.5 Hz can perform reasonably well under slow movement conditions. This filtering will not remove sudden movements which are in the passband. Slower baseline variations such as those induced as a result of breathing movements are removed by the filter.

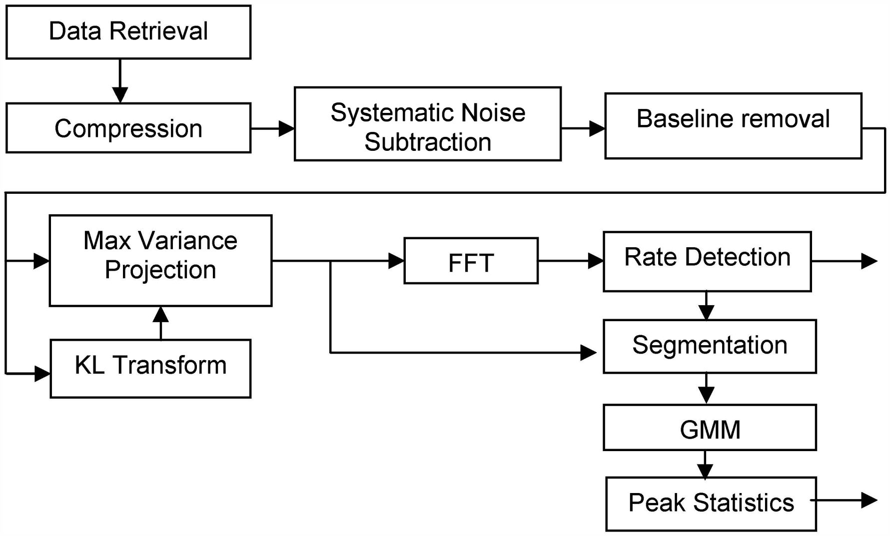

Fig 3. Haptic Lens Image Processing

Let us denote the compressed image data at frame n by $X_c^t(m,n)$, where $X_c^t(m,n)$ represents a 128 by 96 matrix of grayscale pixel data. The output of the baseline removal block is then represented as a convolution:

$$X_{BC}^t(m,n) = \sum_{\tau=0}^{t} X_c^\tau(m,n).h_{HP}(t-\tau) \qquad (1)$$

Where $h_{HP}(t)$ is the impulse response of the high pass filter. We next aim to extract a 1D function of time $x(t)$ from the three dimensional $X_{BC}^t(m,n)$ image data.

Proposed is a scheme utilizing the Karhunen–Loève (KL) transform to obtain $x(t)$ as shown in equation (2):

$$x(t) = w_1^T..\tilde{x}_{BC}(t) \qquad (2)$$

where $\tilde{x}_{BC}$ (t) is a vector obtained by columnization of the matrix $X_{BC}^t(m,n)$, and w_1 is the first eigenvector of the covariance matrix $C_{\tilde{x}} = E\left[\tilde{x}_{BC}, \tilde{x}_{BC}^{\;T}\right]$ corresponding to the largest eigenvalue. Implied in this scheme is the modeling of video data as a stochastic process in time, where projecting the frames onto the first orthonormal basis image w_1 obtained by the KL transform maximizes the variance of the output process $x(t)$. Also implied is the treatment of variance as a measure of information.

It is notable that while simpler approaches such as a simple summation over the image may be feasible in many instances, there are cases where these approaches will not provide sufficient precision. Such is the case where an increased pressure on the membrane of the apparatus causes the liquid to be shifted from one location to another, resulting in a near-zero net pixel brightness effect on the entire frame image. The KL approach in such cases ensures that the relevant data is captured appropriately by assigning negative weights to some of the pixels. The KL transform also emphasizes the image locations where most of the variation is happening, mostly discarding areas unaffected by the heartbeat pulses. Figure 4(a) shows a Haptic Lens sample frame compared to the primary basis image obtained by KL transform used for data extraction shown in (b). It is also worthy to mention that the KL transform will not provide the desired results without a proper baseline removal scheme.

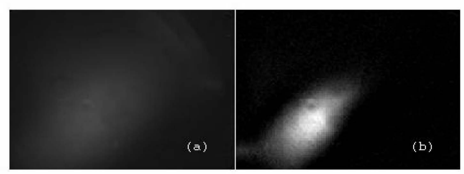

Figure 4. (a) A sample frame indicating the location of impact in the frame (b) Primary basis image obtained from KL transform. Emphasis is brought onto areas with the largest variation in time.

In the following phase the heart rate is derived by first performing a Fast Fourier Transform, followed by a peak search in the interval of 0.7 to 2 Hz (see Fig. 6). Utilizing the heart rate, the $x(t)$ signal is then divided into segments representing each heart beat (see Fig. 7).

The segment separation is performed by finding consecutive minimums separated by heart beat period intervals – as derived from the FFT phase described above –, with a tolerance of 10 percent. The segments are next averaged and fitted to a set of Gaussian Mixed Models with multiple peaks, with each set representing one of the pulse models discussed in Section IV:

$$\bar{x}(t) = \sum_{k=1}^{N_m} \alpha_k.e^{\frac{-(t-\mu_k)}{\sigma^2{}_k}} + v_m(t) \qquad (3)$$

In the above equation $\bar{x}(t)$ represents one heart beat segment obtained by averaging over the individual segments obtained from $x(t)$, N_m is the number of peaks in the m'th pulse model, α_k, μ_k and σ_k are the optimization variables in the fitting process, and finally $v_m(t)$ is the error signal.

The fitting procedure is performed using Nelder-Mead iterative method (see Fig. 8). The mean square of error obtained from each fitting result is computed and compared to decide the pulse model.

VI. Results

In order to validate the Haptic Lens device as a palpation tool for arterial pulse sensing we used the system on 10 people. In order to demonstrate the ease of use of this device and how it can be used by individuals with no medical knowledge or background, we asked people to conduct the experiments themselves. Fig 5 shows an individual using the Haptic Lens to capture their left hand pulse.

Figure 5. Individual using the Haptic Lens

Figures 6-8 show the different stages of the data processing described in Section V on an individual's pulse measurement.

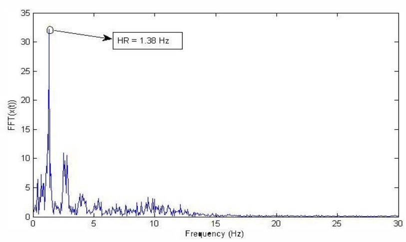

Figure 6. Detecting heart rate from frequency information in x(t).

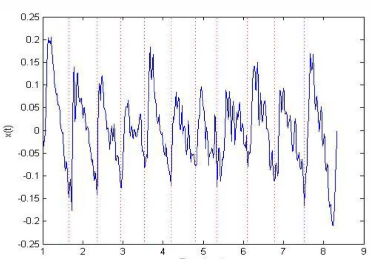

Figure 7. Signal x(t) obtained by projecting the frames onto the primary basis image. The detected segments are separated by vertical dotted lines.

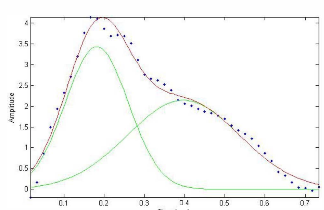

Figure 8. Fitting each individual heart beat segment into a two-peak GMM model.

The system was explained to users as a device for palpating arterial pulse and individuals were asked to adjust the location of the device on their wrists until they could see a pulse-synchronized in the image shown on the computer screen. Once they were satisfied with the position of the device we asked them to hold the device in the same position without moving it for 20 seconds. Figure 9 shows the frequency domain analysis and curve fitting procedures for three selected users.

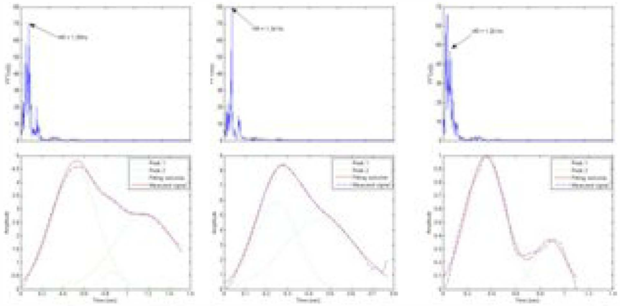

Fig. 9. User Results. Measured Pulse Rates: (a) 1.39 Hz (b) 1.34 Hz, (c) 1.26 Hz.

VII. Conclusion

In this work we demonstrated the use of a novel mechanism for measurement of arterial pressure pulse using the Haptic Lens. We proposed algorithms that show significant pulse information can be extracted from the measurements from the Haptic Lens. In the future, using the 2D capabilities of the Haptic Lens plus faster sampling we hope to create 1D pressure wave propagation parameters over the length of the exposed artery, yielding even more useful data.

References

[1] Michael Sinclair, The haptic lens, ACM SIGGRAPH 97 Visual Proceedings: The art and interdisciplinary programs of SIGGRAPH '97, p.179, August 03-08, 1997, Los Angeles, California, USA.

[2] Xu, L.S., Meng, M.Q., Shi, C., Wang, K.Q., Li, N.M. (2008). Quantitative Analyses of Pulse Images in Traditional Chinese Medicine. Medical Acupuncture, September 20(3): 175-189.

[3] Wu, J.H.; Chang, R.S.; Jiang, J.A. A Novel pulse measurement system by using laser triangulation and a CMOS image sensor. Sensors 2007, 7, 3366-3385.

[4] D. H. Evans and W. N. McDicken. Doppler ultrasound: Physics, instrumentation and signal processing (second edition). Chichester: Wiley, 2000.

[5] Chung-Shing Hu, et al. "Temporal and spatial properties of arterial pulsation measurement using pressure sensor array" Evidence-based complementary and alternative medicine: eCAM, 2011.

[6] Wang BH, Xiang JL. Experiment design and power-spectral characteristics of pulse signal. Chin J Phys Med. 1998;20(3):158–161.

[7] S. Chekmenev, A. Farag, and E. Essock. Thermal imaging of the superficial temporal artery: An arterial pulse recovery model. CVPR, pages 1-6, 2007.

[8] R. Williams, II, M. Srivastava, J. Howell, R. Conatser, Jr., D. Eland, J. Burns, and A. Chila, "The Virtual Haptic Back for Palpatory Training," In Proc. Int. Conf. Multimodal Interfaces, pp. 191-197, 2004

[9] D. Zhang, W. Zuo, D. Zhang, H. Zhang, and N. Li, "Classification of pulse waveforms using edit distance with real penalty," EURASIP Journal on Advances in Signal Processing, vol. 2010, Article ID 303140, 8 pages, 2010.

[10] D.-Y. Zhang, W.-M. Zuo, D. Zhang, H.-Z. Zhang, and N.-M. Li, "Wrist blood flow signal-based computerized pulse diagnosis using spatial and spectrum features," Journal of Biomedical Science and Engineering, vol. 3, no. 4, pp. 361–366, 2010.

[11] Zhou SH, Zhu DZ. The blood dynamics analysis of taut pulse mechanism. Liaoning Journal TCM. 1994;21(21):49–51.